Estimating Pulmonary Arterial Pressure Differences Using Integrated Machine Learning-Computational Fluid Dynamics

Seyed Babak Peighambari[1], Tanmay Mukherjee[1], Rana Raza Mehdi[1], Emilio A Mendiola[1], Reza Avazmohammadi[1]

[1]Department of Biomedical Engineering, Texas A&M University, College Station, TX, USA

Abstract

Pulmonary hypertension (PH) is characterized by a significant increase in mean pulmonary arterial pressure at rest and can initiate substantial right ventricular remodeling, often leading to right heart failure. The diagnosis of PH primarily relies on assessing the hemodynamics of the pulmonary circulation. While non-invasive modalities such as four-dimensional flow MRI and Doppler imaging assist with the diagnosis, PH is confirmed only through invasive right heart catheterization. The challenges of measuring arterial pressures non-invasively have prompted the use of computational fluid dynamics (CFD) models and simulation to assess pulmonary hemodynamics in silico. However, such CFD models have not been widely adopted in clinical practice due to high computational costs and complex deployment procedures. In this study, we introduce a surrogate machine learning (ML) model that circumvents complex CFD methods to predict pulmonary artery differential pressures. A multi-layer feed-forward neural network (MFNN) was trained using the pulmonary branch inlet velocity, alongside pulmonary vascular resistance modeled by the three-element Windkessel formula. The ML model demonstrated remarkable predictive accuracy with an R^2 of 92%. Integrating such a pipeline directly with clinical imaging modalities promises to provide a non-invasive and feasible alternative for assessing pulmonary pressure gradients.

1. Introduction

Pulmonary hypertension (PH) is characterized by a mean pulmonary arterial pressure (mPAP) greater than or equal to 20 mmHg at rest, as verified through right-sided heart catheterization. It impacts around 1% of people worldwide, increases to 10% among those over 65, and affects over half of all heart failure patients [1]. PH is divided into five categories and can arise from various causes such as left heart disease (PH-LHD), lung conditions (PH-lung), and idiopathic issues in the pulmonary capillaries known as pulmonary arterial hypertension (PAH). Diagnosis relies on assessing the hemodynamics of the pulmonary circulation, particulary mPAP and pulmonary arterial wedge pressure (PAWP); an mPAP over 25mmHg is typical across PH forms, and PAWP measurements aid in determining the specific PH type [2].

Clinically, several tools are employed to detect and categorize PH. Echocardiography generally serves as the initial diagnostic test, though its interpretation can be complex due to the remodeling events in the right side of the heart that are often coincident with altered pulmonary pressure [3]. An electrocardiogram (ECG) may support a PH diagnosis, yet a normal ECG does not rule it out. Furthermore, four-dimensional magnetic resonance imaging (4D-MRI) has shown promise in the non-invasive evaluation of arterial hemodynamics, but it alone cannot definitively exclude PH [4]. Right heart catheterization (RHC) remains the gold standard method for directly measuring mPAP and PAWP despite its invasive nature and potentially severe complications in both children and adults. Indeed, RHC can cause major discomfort and pose the risk of complications in children and adults. Thus, the establishment of a non-invasive approach to measuring mPAP and PAWP will make a significant clinical impact in the diagnosis of pediatric and adult PH [5].

Diagnosing PH is complex and often delayed due to vague initial symptoms such as shortness of breath, dizziness, and edema, which typically culminate in severe pulmonary artery and right ventricle (RV) structural changes by the time of diagnosis [2]. Recent studies have aimed at pinpointing early image-based diagnostic markers of PH, exploring MRI and ultrasound metrics such as pulmonary artery mean velocity and distensibility for their possible association with RHC readings [5]. Nevertheless, a precise PH diagnosis still crucially hinges on accurately calculating pulmonary vascular resistance (PVR), calculated from mPAP, PAWP, and cardiac output [2]. The need for invasive RHC as part of early diagnosis underscores the need for a minimally-invasive accelerated approach to more quickly diagnose PH.

The challenges of non-invasively measuring arterial pressures in vivo have spurred the exploration of computational fluid dynamics (CFD) models as tools for assessing hemodynamics via image-based modeling [6]. Advances in computational capabilities now enable detailed CFD simulations of complex, patient-specific arterial structures based on unsteady Navier-Stokes equations. While validated against experimental and clinical data, these models are not yet leveraged in clinical settings due to the high operational costs and extensive preparation they require [7].

In this work, we present a machine learning (ML) model to replace the time-intensive and costly CFD method to predict the pulmonary arterial pressure difference (ΔP). CFD modeling was used with an idealized pulmonary artery bifurcation (PAB) geometry to create a hundred-case synthetic dataset with alternative inlet velocity and PVRs using a 3-element Windkessel formula. The input features, particularly the inlet velocity, were chosen so that they could be obtained from standard MRI or Doppler imaging. Latin hypercube sampling (LHS) [8] was used to generate a varied data set and avoid clustering or repetition in the training data. CFD-derived hemodynamics were used to train a multi-layer feed-forward neural network (MFNN) to predict ΔP. Ultimately, this CFD-ML pipeline, augmented with patient-specific PAB geometry and wall motions, could be advanced to replace expensive and invasive methods for characterizing mPAP.

2. Methods

2.1. Computational fluid dynamics pipeline

An idealized asymmetric PAB geometry, based on averaged anatomical dimensions, was used to create a hundred-case dataset of PAB hemodynamics [9]. In each of the hundred CFD models, a unique static inlet velocity was set in the anatomical range of 0.5-1 (cm/s) [10]. Also, a three-element Windkessel model was designed to represent the PVRs and impose the outflow pressures (Fig. 1A). The three-element Windkessel model is composed of Z, R, and C components representing the PA's impedance, peripheral resistance, and total arterial compliance, respectively [11]. Inlet velocity and the Windkessel parameters were unique in each CFD model; LHS was employed to effectively span the multidimensional distribution of inlet velocity and Windkessel parameters, ensuring a well-distributed and unclustered dataset [8, 12]. The incompressible Navier–Stokes equations with the arbitrary Lagrangian-Eulerian (ALE) formulation were used as the governing fluid dynamics equations, and the continuity and the momentum equations were defined as:

$$\nabla \cdot \mathbf{v} = \mathbf{0}, \tag{1}$$

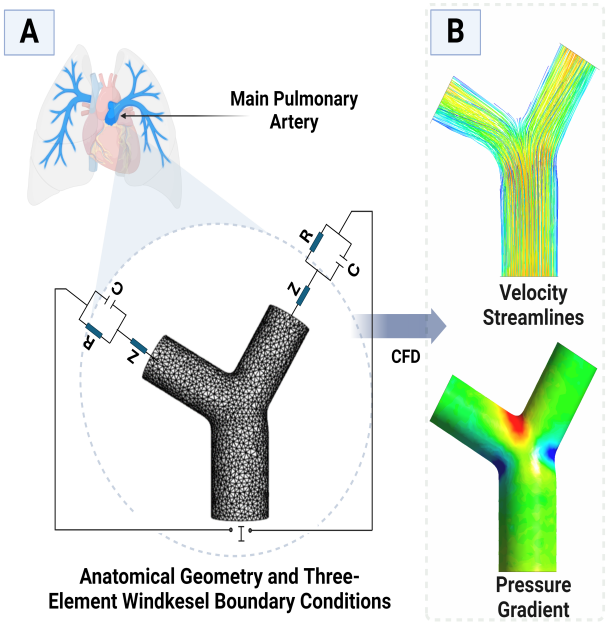

Figure 1. (A) CFD modeling of the main pulmonary artery (PA) branch was used to generate sample data. Inlet velocity and a 3-element Windkessel model were applied as initial boundary conditions, and (B) the resulting velocity streamlines and pressure domain were used to train a machine learning model to predict PA pressure differentials.

$$\rho\left(\frac{\partial \mathbf{v}}{\partial t} + \mathbf{v}\cdot\nabla\mathbf{v}\right) = -\nabla p + \mu\nabla^2\mathbf{v} \tag{2}$$

Here $\mathbf{v}$ represents the flow velocity, and p is the total pressure, while ρ and μ refer to the density and viscosity of blood which were set to 1040 kg/m^3 and 0.0035 $Pa \cdot s$, respectively [13, 14]. Then, CFD modeling produced the inlet and outlet velocities and pressures (Fig. 1B) to be used in training the ML model presented in the next section.

2.2. Machine learning pipeline

We introduced an ML strategy that correlates the defined input variables, including inlet velocity and the Windkessel parameters Z, R, and C, with the output variables, specifically the pressure difference between the PA's inlet and the right and left arterial branches (ΔP). Our ML methodology unfolds in two primary phases, as depicted in Figure 2. Initially, a comprehensive dataset using traditional CFD methods was generated (Fig. 2A). Next, an MFNN was utilized as a sophisticated deep learning mechanism to train the ML model using the CFD data pairs. This approach enabled the application of nonlinear supervised learning techniques tailored to the dataset's non-sequential and non-time-dependent nature [15]. The model was trained on 80 cases, with 20 cases reserved as

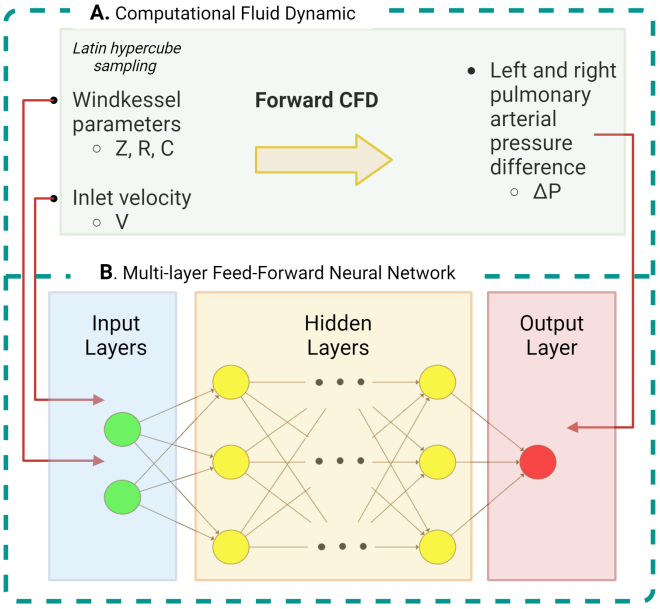

Figure 2. The proposed integrated computational fluid dynamics-machine learning (CFD-ML) pipeline aims to bypass the complexities of traditional CFD modeling. (A) CFD simulations were used to generate data to train the ML model. (B) The trained multi-layer feed-forward neural network ML model predicts pressure differences.

test data. To enhance the model's reliability, we employed 5-fold cross-validation, where the data was divided into five subsets, and the model was iterated five times, each time using a different subset for validation and the remaining subsets for training. This approach ensured a thorough evaluation of the model's performance

3. Results

Using inlet velocity (V), pulmonary arterial impedance (Z), peripheral resistance (R), and total arterial compliance (C) as inputs, the MFNN model was able to accurately predict the pressure differential (ΔP) in both the left and right arterial branches of the pulmonary artery in less than one second on a PC configured with a 2.8 GHz quad-core CPU and 32 GB of RAM. The comparison between the ground truth CFD and the predicted pressure differences for the left and right pulmonary branches across both training and testing datasets showed strong correlations, with testing performance achieving an R^2 score of 92% (Fig. 3). Implementing 5-fold cross-validation and iterating the ML model, the R^2 of training data remained 99% and the predictions on the test dataset demonstrated excellent accuracy with a minimum R^2 score of 92% and a median of 94% (Fig 4).

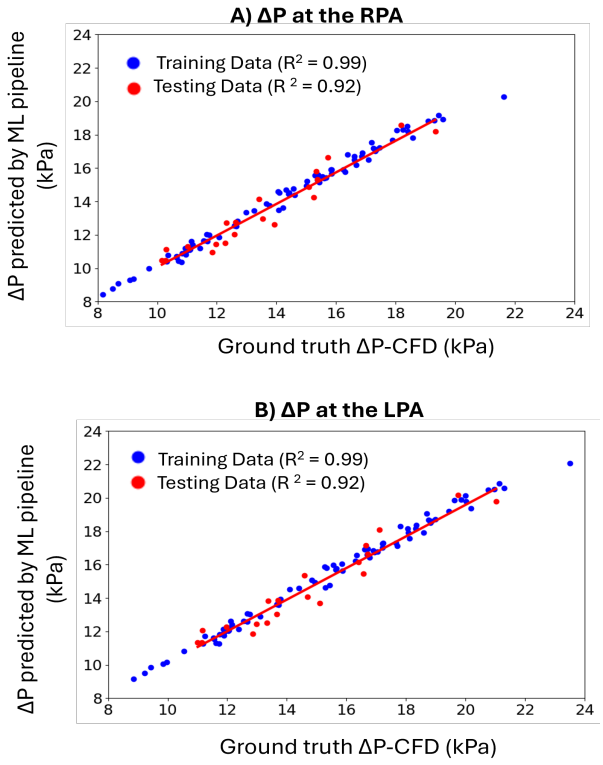

Figure 3. Comparison of the ground truth-CFD pressure difference versus the ML predictions at the (A) right pulmonary artery (RPA) and (B) left pulmonary artery (LPA) branches.

4. Discussions

The definitive confirmation of PH involves the evaluation of the hemodynamics of the pulmonary circulation and requires right-sided heart catheterization to measure pulmonary artery pressures directly. Given the invasive nature of heart catheterization and the crucial role of assessing PA pressures, we introduced an ML model designed to efficiently and precisely predict the pressure difference between the pulmonary artery's inlet and its right and left arterial branches. This model utilizes inlet velocity data, which can be obtained through echocardiography or 4D-MRI imaging techniques, thereby bypassing the need for more complex and expensive patient-specific CFD modeling typically used in such assessments.

Our study consisted of two phases: first, generating a dataset of one hundred CFD cases, and second, applying ML techniques to predict the pressure differences without resorting to labor-intensive CFD processes. The trained ML model was then tested using a dataset not previously encountered during training, where it demonstrated remarkable accuracy in its predictions. In summary, when the ML model is fully trained, there is no need to use the

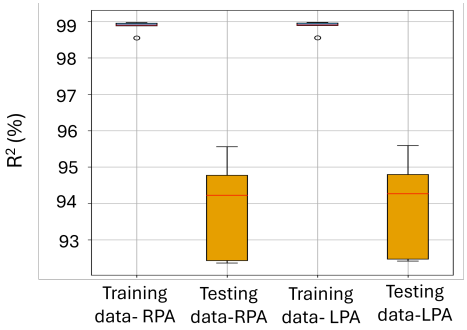

Figure 4. The range of R^2 of the iterated ML predictions of pressure differences in the training and testing data samples at the right pulmonary artery (RPA) and left pulmonary artery (LPA) branches.

arduous CFD modeling to estimate the pressures, and the ML model predicts the pressure differences in less than a second with the minimum accuracy of $R^2 = 92\%$.

Despite its efficiency and accuracy, the current model operates under certain simplifications. Perhaps, most notably, an idealized and fixed geometry was used for training. Future models should be trained on diverse geometric data data, where arterial dimensions can be used as additional input for patient-specific predictions. Also, static flow conditions was assumed as dictated by the Windkessel formula. To enhance accuracy, incorporating a pulsatile flow model would yield more precise results. These advancement will aim to refine the method further, bringing such a tool closer to implementation in the clinical setting.

References

[1] Mandras SA, Mehta HS, Vaidya A. Pulmonary hypertension: A brief guide for clinicians. In Mayo Clinic Proceedings, volume 95. Elsevier, 2020; 1978–1988.

[2] Gali N, Humbert M, Vachiery JL, Gibbs S, Lang I, Torbicki A, Simonneau G, Peacock A, Noordegraaf AV, Beghetti M, et al. 2015 esc/ers guidelines for the diagnosis and treatment of pulmonary hypertension. Polish Heart Journal Kardiologia Polska 2015;73(12):1127–1206.

[3] Yaghi S, Novikov A, Trandafirescu T. Clinical update on pulmonary hypertension. Journal of Investigative Medicine 2020;68(4):821–827.

[4] Swift AJ, Wild JM, Nagle SK, Roldan-Alzate A, François CJ, Fain S, Johnson K, Capener D, van Beek EJ, Kiely DG, et al. Quantitative magnetic resonance imaging of pulmonary hypertension: Practical approach to the current state of the art. Journal of Thoracic Imaging 2014;29(2):68–79.

[5] Vonk Noordegraaf A, Haddad F, Bogaard HJ, Hassoun PM. Noninvasive imaging in the assessment of the cardiopulmonary vascular unit. Circulation 2015;131(10):899–913.

[6] Neelakantan S, Mendiola EA, Vang A, Myers KJ, Zhang P, Choudhary G, Avazmohammadi R. Dissecting contributions of pulmonary arterial remodeling to right ventricular afterload in pulmonary hypertension. BioRxiv 2024;2024–08.

[7] Avazmohammadi R, Mendiola EA, Soares JS, Li DS, Chen Z, Merchant S, Hsu EW, Vanderslice P, Dixon RA, Sacks MS. A computational cardiac model for the adaptation to pulmonary arterial hypertension in the rat. Annals of Biomedical Engineering 2019;47:138–153.

[8] Mehdi RR, Mendiola EA, Sears A, Choudhary G, Ohayon J, Pettigrew R, Avazmohammadi R. Comparison of three machine learning methods to estimate myocardial stiffness. In Reduced Order Models for the Biomechanics of Living Organs. Elsevier, 2023; 363–382.

[9] Berger T, Siepe M, Simon B, Beyersdorf F, Chen Z, Kondov S, Schlett CL, Bamberg F, Tarkhnishvili A, Chikvatia S, et al. Pulmonary artery diameter: Means and normal limits—assessment by computed tomography angiography. Interactive Cardiovascular and Thoracic Surgery 2022;34(4):637–644.

[10] Bouhemad B, Ferrari F, Leleu K, Arbelot C, Lu Q, Rouby JJ. Echocardiographic doppler estimation of pulmonary artery pressure in critically ill patients with severe hypoxemia. The Journal of the American Society of Anesthesiologists 2008;108(1):55–62.

[11] Zambrano BA, McLean N, Zhao X, Tan JL, Zhong L, Figueroa CA, Lee LC, Baek S. Patient-specific computational analysis of hemodynamics and wall mechanics and their interactions in pulmonary arterial hypertension. Frontiers in Bioengineering and Biotechnology 2021;8:611149.

[12] Babaei H, Mendiola EA, Neelakantan S, Xiang Q, Vang A, Dixon RA, Shah DJ, Vanderslice P, Choudhary G, Avazmohammadi R. A machine learning model to estimate myocardial stiffness from edpvr. Scientific Reports 2022; 12(1):5433.

[13] Peighambari SB, Mukherjee T, Mendiola EA, Darwish A, Timmins LH, Pettigrew RI, Shah DJ, Avazmohammadi R. Computational modeling of left ventricular flow using pc–cmr–derived four–dimensional wall motion. BioRxiv 2024; 2024–08.

[14] Peighambari SB, Fatouraee N, Nabaei M, Tavakolian M. Computational modeling of the right ventricular flow based on 2d speckle-tracking echocardiography. In 2020 27th National and 5th International Iranian Conference on Biomedical Engineering (ICBME). IEEE, 2020; 192–197.

[15] Mehdi RR, Kumar M, Mendiola EA, Sadayappan S, Avazmohammadi R. Machine learning-based classification of cardiac relaxation impairment using sarcomere length and intracellular calcium transients. Computers in Biology and Medicine 2023;163:107134.

Address for correspondence:

Reza Avazmohammadi,
Department of Biomedical Engineering, Texas A&M University,
101 Bizzell Street,
College Station, TX 77843,
United States, rezaavaz@tamu.edu